Amphotropic LC Polymers and Their Multilayer Buildup

Kyungsun Choi,[†] Ralf Mruk,[†] Alain Moussa,[‡] Alain M. Jonas,[‡] and Rudolf Zentel*,[†]

Institute of Organic Chemistry, University of Mainz, Duesbergweg 10-14, D-55099 Mainz, Germany, and Unité de physique et de chimie des hauts polymères, Université catholique de Louvain, Place Croix du Sud, 1, B-1348 Louvain-la-Neuve, Belgium

Received June 1, 2005; Revised Manuscript Received August 26, 2005

ABSTRACT: Cationic and anionic LC ionomers, which possess both thermotropic and lyotropic phases, are suitable materials to fabricate multilayers with an internal structure. The LC ionomers were synthesized using a reactive precursor polymer and used for the multilayer buildup by solution-dipping and spin-coating methods based on the electrostatic attraction between polycations and polyanions. Multilayers prepared by the spin-coating method were thicker and showed a smoother surface than the ones prepared by the solution-dipping method. The multilayers prepared by the solution-dipping method showed, on the other hand, a better internal order with respect to layering and orientation of the mesogens, as a result of the liquid crystalline phase. The LC ionomers and multilayers thereof were fully characterized by NMR, UV, IR, DSC (differential scanning calorimetry), XRR (X-ray reflectometry), SPR (surface plasmon resonance), AFM (atomic force microscopy), and polarizing microscopy analyses.

Introduction

The layer-by-layer (LBL) fabrication of molecularly organized film has received tremendous attention in recent years[1,2,11] as a simple, effective, and versatile method to prepare uniform and ultrathin structures. Since composition, thickness, and orientation of each layer can be effectively manipulated using this technique, it provides a route for the formation of various structures layered at the molecular level.[3−7] These manipulations at the molecular level offer many potential advantages in device applications such as active components in nonlinear optical devices (NLO),[4,8] employing materials with selective chemical responses for sensor applications,[7] stable charge-separated assemblies for photovoltaics,[9] and organic light-emitting diodes (OLED's).[10] Since the first report of Decher and coworkers in the early 1990s,[11] there have been numerous reports on the LBL deposition technique based on the electrostatic attraction between polycations and polyanions. Many types of charged molecules and nanoobjects seem are suitable for deposition by the LBL method, but the use of polyelectrolytes rather than low molecular weight polyelectrolytes is advantageous mainly because good adhesion of a layer to the underlying substrate or film requires a certain number of ionic bonds. So far, mostly commercially available polyelectrolytes have been studied, and only in rare cases were functional polyelectrolytes prepared for this purpose.[17,18]

The electrostatic attraction between the oppositely charged polyelectrolytes and especially the entropy gain of the low molar mass counterions are generally thought to drive the depositions. The amount and conformation of adsorbed chains depend on dramatically processing parameters, particularly ionic strength and pH of the deposition solution, as well as the charge densities of both polyelectrolytes. A number of articles have explored the electrostatic parameter in order to delineate conditions of polyelectrolyte multilayer film formation and to correlate molecular and processing parameters with the final film structure.[12−15]

Concerning the multilayer buildup by the LBL technique, there is a general interest in obtaining multilayers with an internal structure.[19] However, multilayers prepared by LBL usually present a low degree of internal organization, and this may be a limitation of the technique. Well-organized multilayers would be advantageous for the applications mentioned, especially for those requiring a vectorial transfer of energy, electrons, or matter or when a precise placement of active functional groups in confined layers is desired. Usually, multilayer films prepared by the LBL method show a strong interpenetration between the oppositely charged polymer layers. Because of this interpenetration, these multilayer films do not contain defined internal sublayers, and no Bragg peaks are observed by grazing angle specular scattering measurements (X-ray reflectometry, XRR, or neutron reflectometry, NR).[19,20] Several attempts have been presented to use multilayers containing rigid ionic blocks for reduction of interpenetration in order to observe Bragg peaks. However, very particular conditions seem to be necessary, but still the appearance of Bragg peaks is exceptional.[19−23]

To get multilayer films with well-defined internal structure, we have studied multilayers of ionic liquid-crystalline (LC) polyelectrolytes by LBL.[24,25,36] However, even in the case when both anionic and cationic LC ionomers showed a smectic phase—as neat material—in their bulk state, no Bragg peaks could be detected for the multilayers prepared by the LBL technique.[36] This might be explained by the fact that thermotropic liquid crystals show only liquid-crystalline properties in bulk and not in solution. Accordingly, LC ionomers do not show any liquid-crystalline properties during the adsorption from solution. After ion pairing, the formation of the liquid-crystalline order is not possible because of the low mobility inside the polyelectrolyte complex. As a consequence, it seems desirable to investigate novel LC polyelectrolytes, which preorganize in solution through a lyotropic LC phase (high mobility) prior to drying a thermotropic LC phase (bulk state); thereby,

[†] University of Mainz.
[‡] Université catholique de Louvain.
* Corresponding author. E-mail: zentel@uni-mainz.de.

10.1021/ma051131t CCC: $30.25
Published on Web 10/01/2005

Scheme 1. Synthesis of the Mesogen-Containing Primary Amine

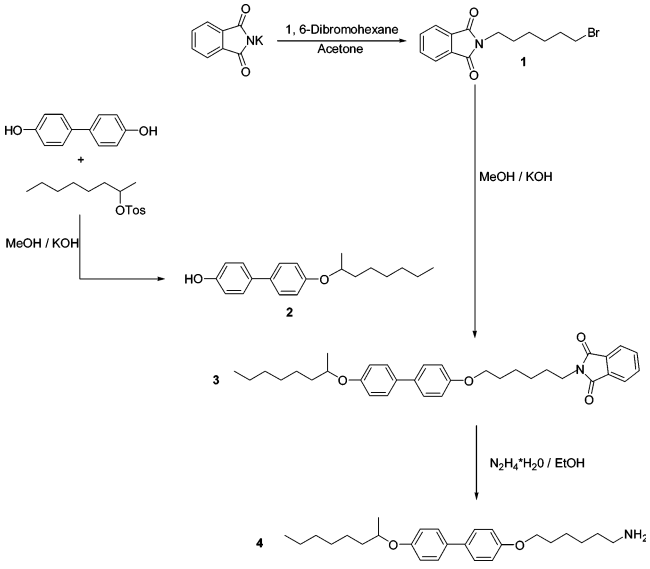

LBL multilayers with internal order may be achieved. After the removal of the solvent, these lyotropic phases change into thermotropic phases, which can stabilize the internal structure within the dried multilayer film.

In this paper, we describe the synthesis of such new LC ionomers, possessing an amphotropic character.[37] The polymers show both thermotropic phases in bulk and lyotropic phases in concentrated solution. They can be used for the multilayer buildup by LBL (solution-dipping) and self-assembly spin-coating (spin-coating) method.[27] X-ray reflectivity measurements indicate internal layering in multilayer films, and angular dependent UV/vis measurements present a preferred orientation of the mesogens perpendicular to the surface.

Results and Discussion

Synthesis of the Amphotrophic Polymers. The chemical structures and reaction schemes of the LC polymers and ionomers prepared in this study are shown in Schemes 1 and 2. The new LC ionomers **P2** and **P3** were synthesized by a reaction of a biphenyl-functionalized amine and ionic amines with a reactive precursor polymer (Scheme 2). The side groups (ionic groups and mesogens) are attached to the main chain by amide bonds which are stable against hydrolysis. The mesogens consist of a long alkyl chain to increase the amphiphilicity of the structure. Branched alkyl chains are used to prevent side-chain crystallization. A larger variety of polymers, which are synthesized under the variation of concentration of mesogens and ionic groups, were briefly described elsewhere.[26] Here we selected homopolymer **P1**, the anionic LC ionomer **P2**, and the cationic LC ionomers **P3a,b**. First, the mesogen-containing primary amine **4** had to be synthesized, as shown in Scheme 1. Phthalimide potassium, which was transformed into the corresponding *N*-(6-bromohexyl)-phthalimide **1**. The phenol **2** was obtained by reaction of 4,4′-dihydroxybiphenyl and racemic *p*-toluenesulfonic acid-2-octyl ester. Compounds **1** and **2** were afterward reacted to obtain the phthalimide protected primary amine **3**. In the final step, the protection group was then cleaved by treatment with hydrazine hydrate in ethanol, yielding 60% of **4**.

The synthesis of the polymers started with the polymerization of *N*-acryloyloxysuccinimide.[28−30] To determine the molecular weight, the reactive ester polymer was reacted with an excess of *N*-methylhexylamine. The resulting polymer was analyzed by GPC with THF as eluent; a M_n of 28 000 g/mol and a M_w of 49 000 g/mol were found.[37]

For the synthesis of the LC polymers (Scheme 2), the reactive ester polymer was reacted, at first, with the primary amine **4** (slight excess for homopolymer **P1** and varying amounts for the LC ionomers **P2** and **P3**). The completeness of the reaction was checked by thin-layer chromatography. For the synthesis of the LC ionomers **P2** and **P3**, afterward, an excess of 4-aminobutyric acid methyl ester hydrochloride or 4-amino-1-triethylphosphoniumbutane dihydrochloride was added, respectively. The resulting nonionic polymer was precipitated and dried. Finally, the anionic ionomer **P2** was created by hydrolysis of the ester group (Scheme 2 and Experimental Section), and in the case of the cationic side chains of the polymer, **P3** was already ionic. The incorporation of biphenyl-containing side chains in polymer **P2** was confirmed by UV/vis spectroscopy measurements. 50% of the polymer side chains contain biphenyl mesogens, corresponding to the amount of the biphenyl-containing primary amine used for the polymer analogous reaction.

Liquid Crystalline Behavior. The LC phases of **P1**−**P3** were characterized by polarizing microscopy, differential scanning calorimetry (DSC), and X-ray reflectivity measurements. The polymer melts and especially the ones from the LC ionomers **P2** showed a rather high viscosity, which might be explained by the fact that H-bonding of amide groups reduces mobility. For **P2** and **P3** in addition the formation of ion pairs has to be considered (see ref 36 for similar observations), which are especially strong for the carboxylate groups. Nevertheless, LC phases with smectic textures (batonetts)[41] were observed for all polymers by polarizing microscopy after prolonged annealing (see Figure 1a). For **P1** the clearing temperature was 163 °C. In the series of the cationic LC ionomers (**P3a**,**b**), the decreasing temperature decreased with increasing amount of the bulky triethylphosphonium groups (see ref 36 for similar behavior). A different effect was observed for **P2**. The clearing point was higher than 200 °C and occurred at decomposition. This happens presumably because of a strong tendency of the small carboxylate groups to demix from the hydrophobic mesogens (see X-ray measurements and Figure 2). As a result, this segregation stabilizes the smectic phase. The phase transition temperatures are included in the reaction scheme 2.

X-ray reflectivity measurements showed a smectic layer spacing of 48.5 Å for **P1** and of 72 Å for the LC ionomer **P2** in bulk state. Based on the molecular model presented in Figure 2a, these spacings correspond to an interdigitated smectic structure for the homopolymer **P1** (smectic layer thickness is about 1.6 times the length of the mesogen, which is 30 Å) and a bilayer structure for the LC ionomer **P2** (distance from end of mesogen to the ionic group is ∼39 Å).[42,43] The difference between the "ideal" bilayer length of 78 Å and the experimentally determined length of 72 Å can be explained due to partial coiling, some tilting of the mesogens, and/or a partial interdigitation of the ends of the alkyl chains. The bilayer structure is a result of the segregation between the hydrophilic ionic groups and the hydro-

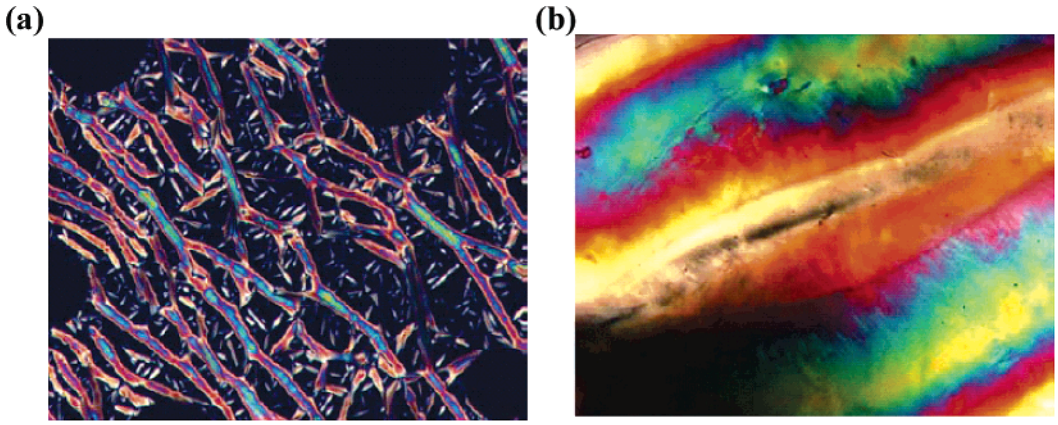

Figure 1. Polarizing microscopy image of (a) a thermotropic phase of **P1** (163 °C) and (b) a lyotropic phase of **P3b** (50 °C) with ethylene glycol.

Scheme 2. Structures of Mesogen-Containing Polymers (s: Smectic Phase; i: Isotropic Phase)

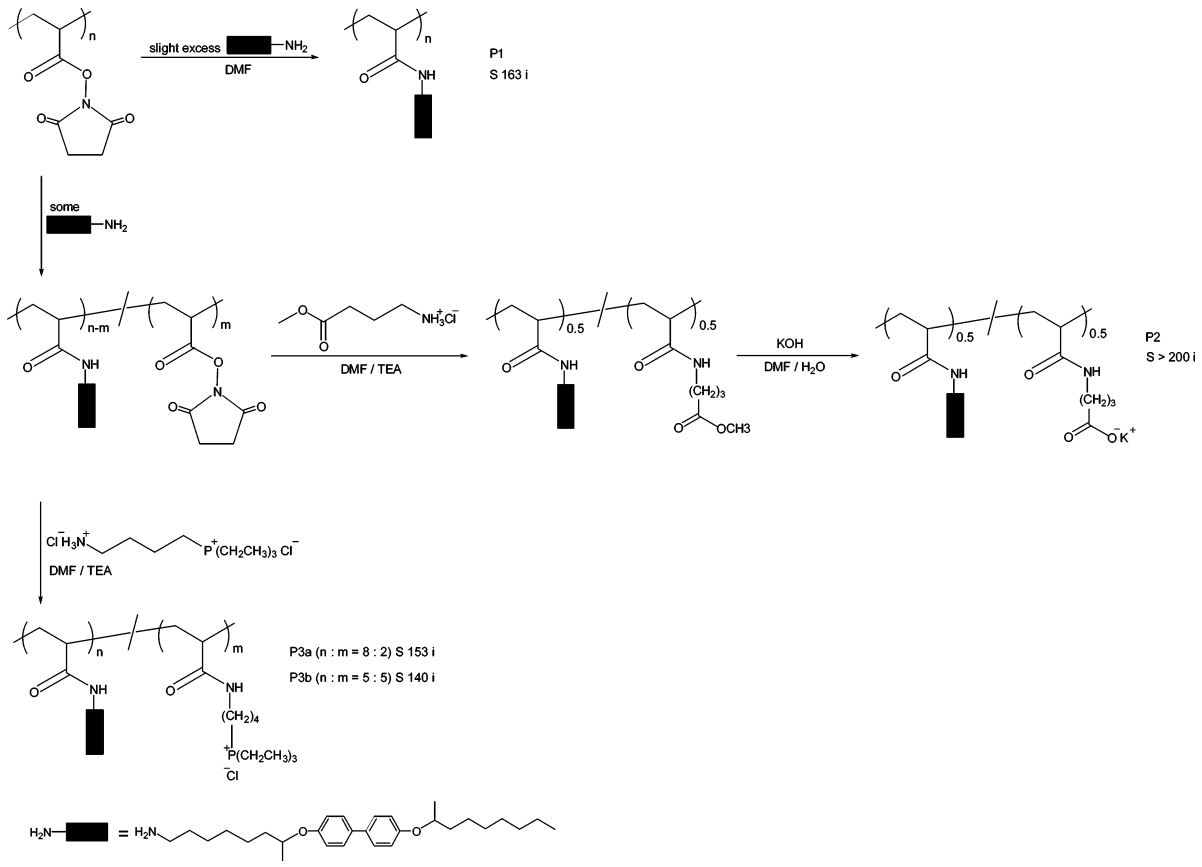

phobic mesogens. It is the precondition for the formation of a lyotropic phase in polar solvents. **P2** and **P3b** do not dissolve in water; only slight swelling can be observed, while preserving their liquid crystalline phase. To prove their potential to form lyotropic phases in polar solvents, ethylene glycol was used as polar solvent. Contact preparations in ethylene glycol show clearly the formation of lyotropic phases at high concentrations of **P2** and **P3b** (see Figure 1b). The observation of lyotropic phases has also been made for a large variety of other LC ionomers of similar structure.[26,37] As a result, **P2** and **P3b** are amphotropic polymers, which form both thermotropic smectic phases in the bulk and lyotropic phases in polar solvents, such as ethylene glycol.

Multilayer Buildup. After analysis of the phase behaviors of the LC ionomers **P2** and **P3b**, the multilayer buildup with oppositely charged polyelectrolytes was successfully examined using the method introduced by Decher.[11] For **P2**, a comparison between the LBL solution-dipping method and the subsequent spin-coating method[31−34] was done. For both processes, **P2** and **P3b** were dissolved in THF with the addition of some ethylene glycol or water (5:1 ratio), and in this solvent mixture, no lyotropic phases are formed. During the drying procedure, THF evaporates first, increasing the concentration of ethylene glycol or water to a range, where lyotropic phases can be expected. Before alternately depositing polymer **P2** (anionic LC ionomer) and poly(choline methacrylate) (PCM) or poly(2-acryloylamino-2-methylpropyl sulfonate sodium salt) (PAMPS) and **P3b** (cationic LC ionomer) onto the substrate, poly(ethylenimine) (PEI) and PAMPS were predeposited two times as basis layers.

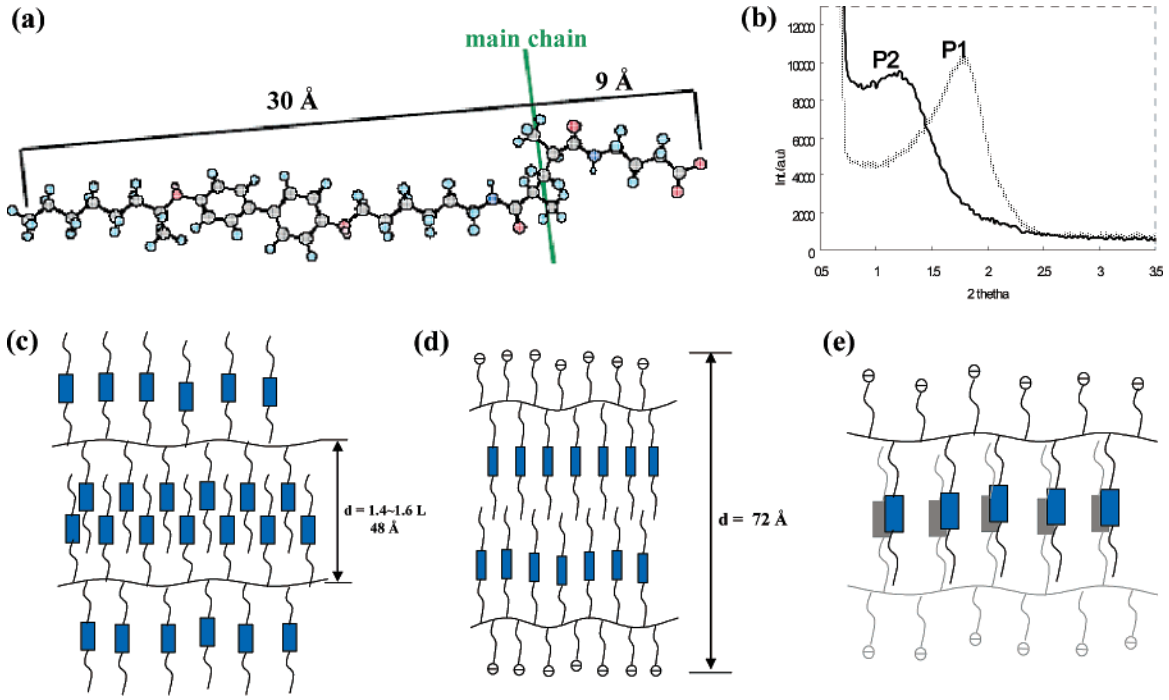

Figure 2. (a) Molecular model structure with distance of **P2** by using Chem 3D Ultra 7.0. (b) X-ray scattering diagram of **P1** (homopolymer) and **P2** (anionic LC ionomer) in bulk state (using Ni-filtered Cu Kα radiation, λ = 1.54 Å). (c) Schematic representation of the smectic bulk structure of **P1** and (d) **P2**. (e) Interdigitated layer structure present in the multilayer.

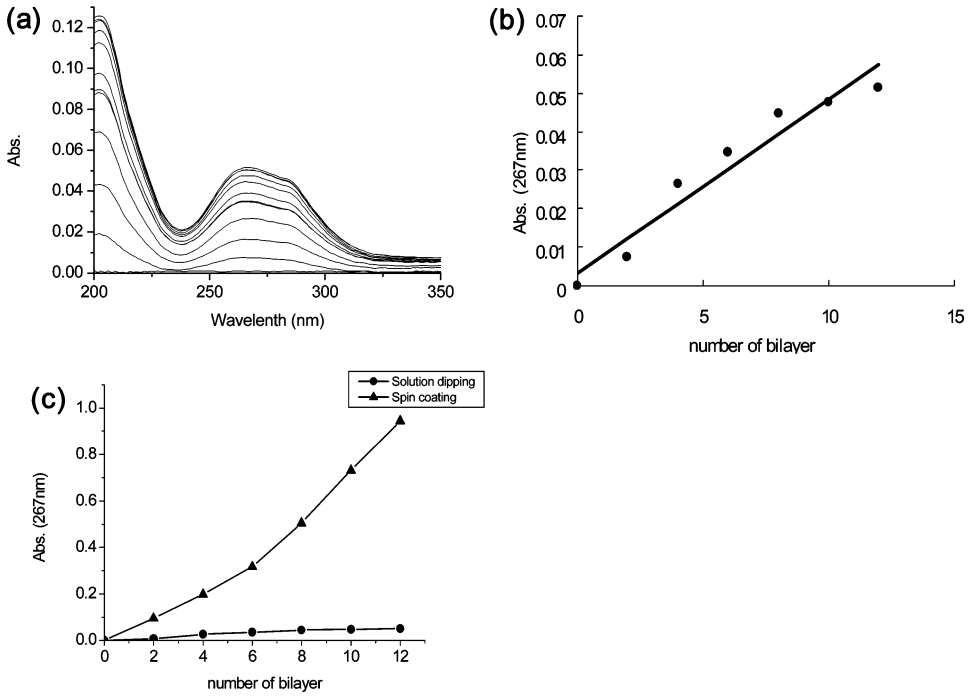

Figure 3. Multilayer buildup from LC ionomer **P2**. (a) UV/vis spectra measured during the multilayer buildup of **P2** and **PCM** by solution-dipping. (b) Growth of the solution-dipping films at 267 nm. (c) Comparison of the growth of the multilayer films assembled by solution-dipping (●) and spin-coating (▲).

For a comparative study, multilayers were assembled using solution-dipping as well as spin-coating methods applying the same conditions. The preparation of multilayer assemblies based on the solution-dipping method was achieved by dipping the substrate alternately for 10 min in cationic aqueous solution of PCM and then in anionic polymer **P2** solution and rinsing three times with plenty of Milli-Q water fir 1 min between these two steps. A similar procedure was adopted when assembling the multilayers by the spin-coating method. The polymer solution and the aqueous solution of PCM were poured onto a substrate, and then the substrate was spun at a speed of 4000 rpm for 15 s.

Figure 3a showed the multilayer buildup from LC ionommer **P2** investigated by UV/vis; the increase of the maximum of the $\pi-\pi^*$ absorbance of the biphenyl mesogen at 267 nm as a function of the number of bilayers for both the solution-dipping and spin-coating multilayers, respectively. According to Figure 3b, the deposition process was linear, indicating that the amount of material deposited per bilayer is completely reproducible from layer to layer. Similar behavior of the multi-

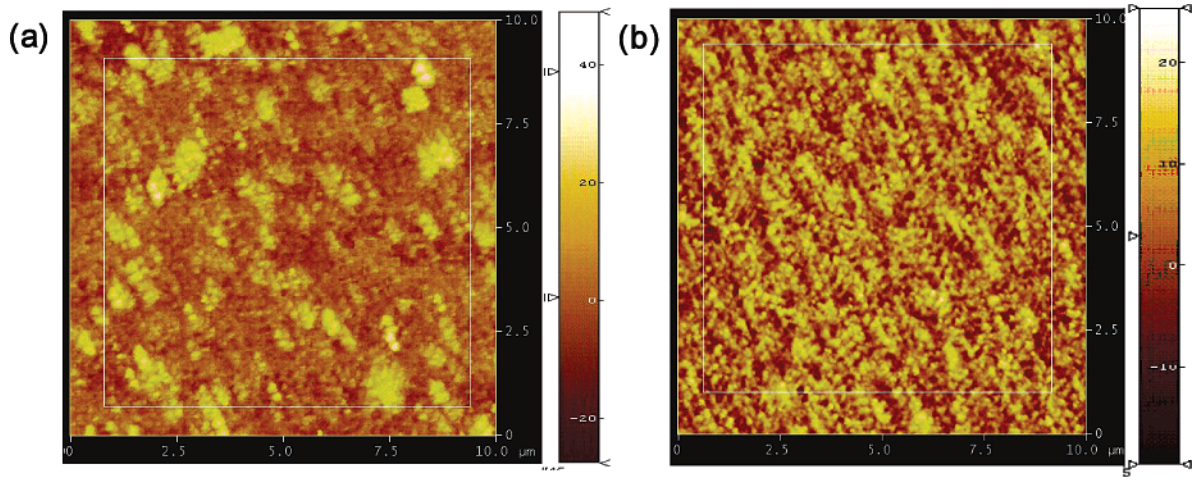

Figure 4. Tapping mode AFM images of 12 double layers of **P2** and PCM multilayer films prepared by (a) the solution-dipping method and (b) the spin-coating method.

layer buildup using the spin-coating method was investigated as well. Thus, with both methods, it is possible to prepare multilayers, which grow constantly in thickness according to the number of bilayers. Figure 3c showed the difference in UV/vis absorbance of multilayer films with alternating **P2** and PCM layers prepared by solution-dipping and spin-coating methods. It is obvious that the absorbance of the spin-coated films was about 20 times as high as those prepared by solution-dipping. This happens despite the fact that the spin-coated film was adsorbed onto only one side of a quartz substrate, while the film prepared by the solution-dipping method was adsorbed onto both sides of a quartz substrate. This was in agreement with literature data.[27,31–33] With regard to the formation of an internal order, both types of films could be different: This significant difference of the absorption between the multilayers from the solution-dipping and the spin-coating method was caused by the different adsorption mechanisms. During the solution-dipping process, LC ionomer chains diffused toward the substrate, and then the adsorbed chains rearranged themselves on the surface. After evaporation of the THF, during the drying process, the concentration of polymers in the water phase increased, whereby the formation of a lyotropic phase was expected. This drying process was quite slow, and it can provide enough time to rearranged adsorbed LC ionomers and to oriented mesogens during the drying process. Subsequently, solution-dipping samples had preferably structured order due to the oriented mesogens, and it would be perpendicular to the surface.

On the other hand, the spin-coating method results in thicker films. In the spin-coating process, the adsorption and rearrangement of adsorbed chains on the surface and the elimination of weakly bound LC-ionomer chains from the substrate are almost simultaneously achieved at a high spinning speed for a short time. A very fast elimination of the solvent yields thick layers. Quick solidification and polyelectrolyte formation compete with the ordering process. With regard to the formation of an internal order in the multilayer system, the film of the spin-coating method may possess less well-ordered internal structures than that of the solution-dipping method.

To investigate the difference between both types of multilayers in more detail, they were characterized by surface plasmon resonance (SPR, thickness), atomic force microscopy (AFM, roughness, topology), X-ray reflectometry (XRR, internal order), and angular dependent UV/vis measurements to monitor the order within the multilayers. AFM images can give information about the surface coverage and roughness of the assembled multilayers. These AFM images were taken in air at room temperature in the tapping mode on multilayer samples prepared by solution-dipping and spin-coating on quartz (12 double layers each). The results are displayed in Figure 4.

A clear difference can be seen between the solution-dipped (Figure 4a) and the spin-coated sample (Figure 4b). The solution-dipped sample showed relatively large flat plateaus, separated by sharp steps, whereas the spin-coated sample showed a smoother variation of the height and a finer structure. As a result, the surface roughness (standard deviation from average) of a solution-dipped film is about 5.9 Å and that of a spin-coated film only 3.7 Å. This demonstrates that the shear forces during the spinning process enhance the planarization of the multilayer film. On the other hand, the solution-dipped sample resembles the thin films of smectic liquid crystals,[38–40] which display also large plateaus separated by sharp layer steps.

To determine the thickness of the multilayer films, surface plasmon resonance (SPR) measurements were performed at various stages during the solution adsorption process (solution-dipping).[35] For the much thicker samples obtained by spin-coating method a proper evaluation was not possible. Examples of SPR curves are depicted in Figure 5. Measurements were performed after adsorption of each bilayer from THF/water mixture onto a thin gold film, which was brought into optical contact with a prism afterward. Then the reflectivity of the sample is monitored as a function of incident angle Θ (see Figure 5).

The shift in the SPR angle (minimum of curve) observed during the formation of the multilayer (**P2** and PCM) can be used to determine the film thickness, if the refractive index of the film is known. As a starting point, we assumed the refractive index of LC-ionomer **P2** to be 1.5, as generally used.[35] A value of about 6 Å was found for the initially adsorbed anionic layer of 3-mercaptopropionic acid used to functionalize the metal gold layer. The resulting evaluation (Figure 5b) showed a linear thickness increase with a thickness per bilayer (cationic layer (PCM) and anionic ionomer layer (**P2**))

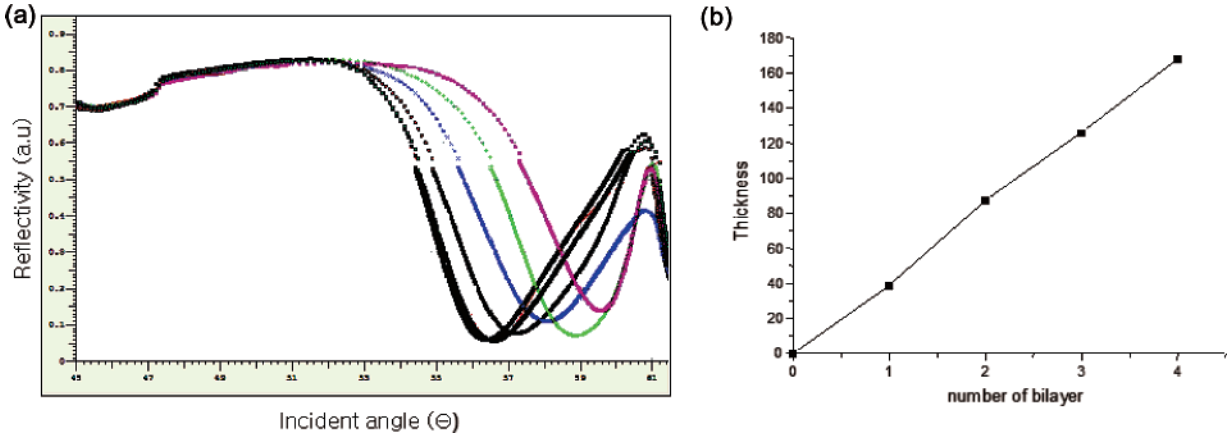

Figure 5. (a) Angular dependent SPR curves after different deposition cycles of the LC polymer **P2** and PCM by the solution-dipping method. (b) The film thickness according to the number of bilayers.

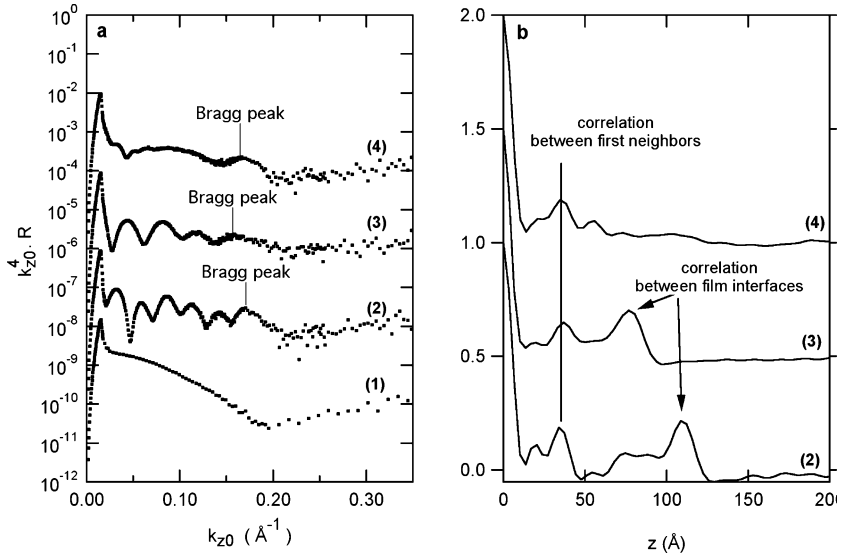

Figure 6. (a) X-ray reflectivity of different multilayer films: (a-1) basis double layer prepared with PEI and PAMPS; (a-2) 16 bilayers sample with **P2**/PCM prepared by the solution-dipping method; (a-3) annealed solution-dipping sample for 12 h at 150 °C; (a-4) 16 bilayers sample with **P2**/PCM prepared by the spin-coating method. k_{z0} is the vertical component of the incident photons in a vacuum. (b) Patterson function of samples shown in (a). In (a) and (b), the curves are shifted vertically for clarity.

about 40 Å. This value per double layer is rather high compared to "usual" polyelectrolytes, but still it is in the range of values found for other LC ionomers.[24,25,36] This is a consequence of the low charge density of the rather hydrophobic LC ionomers.

The question to be answered is: Is there an influence of the liquid-crystalline phase on the adsorption process? SPR measurement gives only an averaged thickness of the adsorbed film. Following the arguments of the introduction (difficulty of complete reorganization of polyelectrolyte multilayer assembly; preorganization in lyotropic phase), there should be a relation between the smectic structure and the thickness of the adsorbed layer. On the basis of the X-ray results of **P2** and the molecular model (see Figure 2), a thickness of about 80 Å would have been expected per adsorbed double layer of LC ionomer and polycation (an anionic smectic double layer of **P2** and some thickness for the cationic PCM layer). However, the thickness of the double layer adsorbed from solution is only half as thick (40 Å, SPR). Concerning the alternating deposition sequence in multilayer buildup between **P2** and PCM, the **P2** layer must expose negative charges to both sides as presented in Figure 2e. A possibility to combine a thickness of 40 Å per double layer, fabricated between polycation and polyanion, and a smectic structure is the assumption of the adsorption of fully interdigitated monolayers of **P2** (see Figure 2e). That is to assume a structure in the multilayer, which is different from the double layers stable in the melt. Such fully interdigitated monolayers result if mesogens are originating from different polymer chains interdigitate, as found for homopolymer **P1**. The mesogens may pack well in such an arrangement, but the distance between the ionic groups must be increased compared to the situation in bulk (Figure 2). This might be possible in the lyotropic phase due to the presence of solvent.

To determine of the order within the multilayer assembly, X-ray reflectivity measurements were made. For these measurements, samples were made differently that they consisted of 16 bilayers, and they were assembled on a polished silicon wafer. The results obtained from solution-dipped and spin-coated samples are displayed in Figure 6.

The evaluation of the X-ray reflectivity measurements shows for all samples a weak Bragg peak at a k_{z0} value of about 0.17 Å^{-1}, suggesting an internal ordering. We assume that this is the second order of a Bragg peak located at about $k_{z0} = 0.085$ Å^{-1} and buried below Kiessig fringes. This would correspond to a layering of

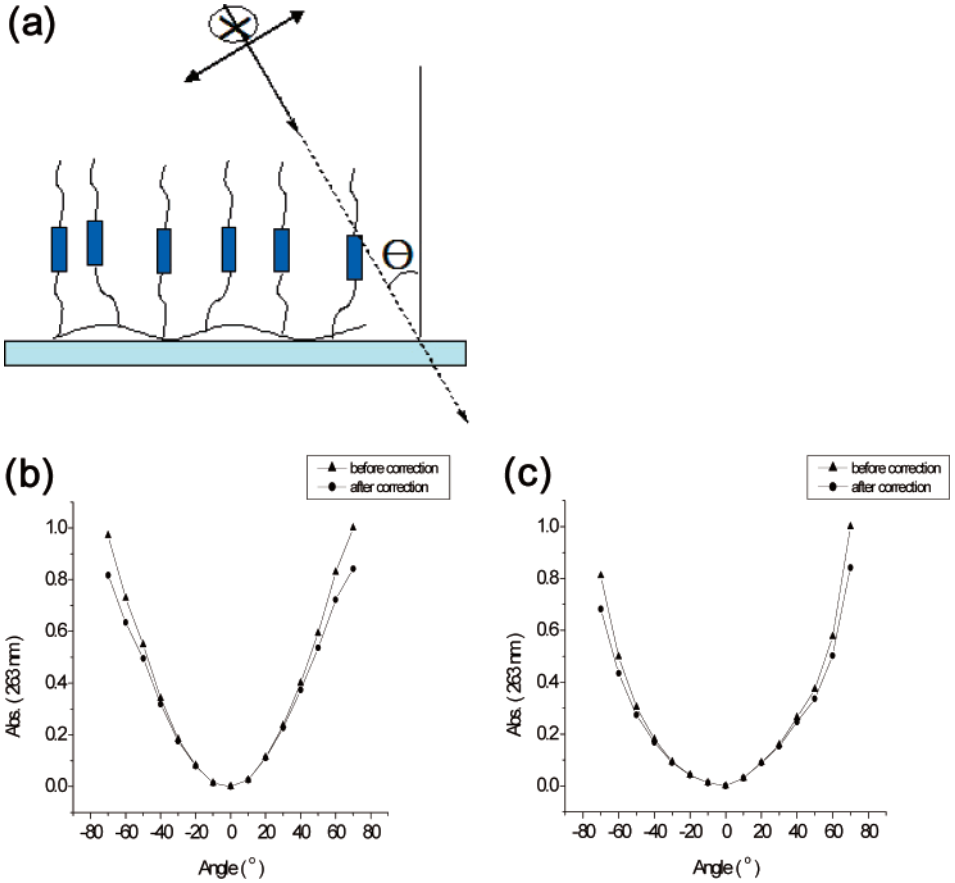

Figure 7. (a) Geometry scheme for the angular dependent UV/vis measurement with unpolarized light, i.e., light polarized within the paper plane and perpendicular. Note that the absorption of light polarized perpendicular to the paper plane should not vary while changing the angle Θ. (b) Results of angular dependent UV/vis measurement of 12 bilayers consisting of **P2** and PCM prepared by the solution-dipping method and (c) by the spin-coating method. For comparison of the both spectra the absorption perpendicular to the substrate $A_\perp$ was subtracted. ▲: primary data; ●: after thickness correction by factor d.

about 37 Å, in agreement with the values of the increment determined by SPR measurements. To check this hypothesis, we have computed the Patterson functions from the X-ray reflectograms, as described previously.[19] The Patterson function $P(z)$ is proportional to the probability of finding in the film two interfaces spaced apart by a distance z. For all **P2**-based samples, a strong peak develops at 36 Å in the Patterson functions, indicating the existence of a periodic fluctuation in the film. Indications for correlation between second neighbors can also be seen in these functions. This inner periodic fluctuation is found independent of the preparation of the sample. It is, however, better developed for the sample obtained by solution-dipping, and it decreases during annealing. Nevertheless, these experiments clearly demonstrate that layering exist in all **P2**-based films, albeit of limited spatial extent. Next, only samples obtained by solution-dipping show Kiessig fringes. These fringes transform in the Patterson function into a final peak whose position directly determines the film thickness. This shows that the films from the solution-dipping method are flat and smooth. However, the thickness of the films prepared by the solution-dipping method is much lower than expected, indicating incomplete growth on the silicon wafer. Interestingly, the film contracts upon annealing; its thickness decreasing from 109 to about 77 Å, testifying for substantial rearrangements occurring upon annealing. By contrast, the film prepared by spin-coating does not present Kiessig fringes or a strong final peak in the Patterson function. Since the outer surface of this film was shown to be very flat by AFM, the absence of Kiessig fringes most probably results from a very large film thickness, which prevents to get fringes due to the finite resolution of the X-ray reflectometer.

As a smectic layering exists, the mesogenic groups should be oriented perpendicular to the surface. UV/vis dichroism offers a possibility to determine the order parameter of the mesogens by angular dependent UV/vis measurements, using unpolarized light. These were done with the multilayer samples obtained by solution-dipping and spin-coating methods. The results are displayed in Figure 7. In addition, it must be noted that the measurements were repeated with same samples after 6 months. The samples were stored at room temperature without special precaution, and we can conclude that the samples do not change. This proves that a stable orientation in multilayer is achieved.

First, the measurements had to be corrected for the absorbance by a correction factor d (see Experimental Section). The corrected values showed a strong increase of the absorption on increasing the angle, too. As the biphenyl chromophores absorb light polarized along their long axis, this proved that the biphenyl units were oriented preferably perpendicular to the surface.

As the measurements were carried out with unpolarized light (Figure 7a), 50% of the light is always polarized perpendicular to the long axis of the biphenyl chromophores independent of the angle. The absorption of the other 50% of the light (polarized within the paper plane of Figure 7a) should follow eq 1. With this equation the angular dependence of both types of

samples can be fitted for angles from −50° to +50°. From the fit, $A_{||}$ (parallel absorbance) and $A_{\perp}$ (perpendicular absorbance) were obtained (see Experimental Part). Using these results, it was possible to estimate the nematic order parameter S (quality of the orientation of the long axis of the biphenyl chromophores perpendicular to the surface) using eq 2.[44] As a result, an order as high as $S = 0.25$ was obtained for the sample prepared by solution-dipping, and a value of only $S = 0.07$ was obtained for the sample obtained by spin-coating. In LC phases, typical order parameters between 0.3 and 0.6 are found for nematic phases and 0.6 and 0.8 for smectic phases.[43,44] Consequently, the value observed for the solution-dipped sample is very close to the value of monodomain liquid crystalline phases, and the value for the spin-coated sample corresponds only to "some" preferred orientation.

$$A(\Theta) = \sqrt{A_{||} \sin^2 \Theta + A_{\perp} \cos^2 \Theta} \quad (1)$$

$$S = \frac{A_{||} - A_{\perp}}{A_{||} + 2A_{\perp}} \quad (2)$$

Conclusions

In this work, new amphotropic LC ionomers, which possess smectic thermotropic phases in bulk and lyotropic phases in solution, were synthesized. These LC ionomers could successfully be used for the multilayer buildup by solution-dipping and spin-coating methods. Although both methods showed quite linear and reproducible multilayer buildup performances by UV/vis measurements, the AFM, SPR, and XRR measurements indicated differences between multilayer samples prepared by both methods. The differences between the solution-dipped and spin-coated samples can be rationalized by the different mechanisms.

During the solution-dipping process, the charged LC ionomers diffused toward the substrate, and then adsorbed chains rearranged themselves as thin films. The amount of adsorption is controlled by charge compensation, and the whole deposition process (including final drying) is quite slow. It gives enough time to orient mesogens in the lyotropic phases. After removal of the solvents, the lyotropic phases (in concentrated solution) change into thermotropic phases (in bulk), resulting in a stabilized internal structure. The orientation of the mesogens is well improved due to the liquid crystallinity. However, the amount of the adsorbed LC ionomers will—in most cases—not be the exact amount needed to form the smectic layers; thus layer steps arise. As a result of a lyotropic phase, which is different from the thermotropic bulk phase (monolayers vs double layers), the films rearranged during annealing, decreasing the order and flatness of the films.

On the other hands, the spin-coating method gave much thicker films due to the fast elimination of the solvent and the high spinning process. In addition, spin-coated films possessed less internal order. The drying process happens very quickly, and it provides not enough time for the formation of the LC phase. Thus, the surface of the film was smoother because it does not fabricate the smectic layer. At the same time, the LC order, with respect to both layering and parallel orientation of the mesogens, was poorer compared to the solution-dipped sample.

The questions remaining are: What is the relation between the bulk phase of the LC ionomers and the structure present in the multilayers? And how is their long-term stability?

At first, a direct comparison of the LC behavior of multilayers and the bulk or lyotropic phase of the LC ionomer is impossible because of the different composition. The LC ionomer contains low molar mass counterions in both bulk and lyotropic phase; on the other hand, the multilayer contains polymeric counterions (the polycation). Thus, from a thermodynamic point of view the phase behavior should be different, and the LC phases of the multilayer have to be compared to that of a one to one mixture of LC ionomer and the polyelectrolyte. Now, the one-to-one composition from polycation and polyanion—present in the multilayers—corresponds to a polyelectrolyte complex, in which the viscosity is extremely high and the equilibrium is hardly reached. If e.g. LC ionomer and poly(choline methacrylate) (PCM, polycation) solutions are mixed, an unmeltable polyelectrolyte complex is formed immediately. So there is no equilibrium reference state for a bulk phase of the mixture, to which the multilayers can be compared. In addition, no equilibrium state is reached for the multilayer, too. On the contrary, the structure present during adsorption and drying (lyotropic phase, transition to thermotropic bulk phase) is frozen-in. This structure is, however, long-term stable. This can be shown e.g. by a repetition of the angular dependent UV measurements done with samples stored at room temperature for 6 months, which reproduced the old parameters.

Consequently, we obtained multilayers with synthesized amphotropic LC ionomers, which are suitable materials to fabricate internal ordered multilayers. The multilayers deposited by the solution-dipping method show the order parameter closed to that of real liquid-crystalline monodomins, and based on that parameter, the mesogens of the LC ionomers are oriented perpendicular to the substrate.

Experimental Section

LC Polyelectrolytes. *N-(6-Bromohexyl)phthalimide* **(1).** A solution of 1,6-dibromohexane (44.8 g, 0.183 mol) in 300 mL of acetone was heated to reflux. Potassium phthalimide (17 g, 0.092 mol) was added in four portions over a period of 4 h. The resulting mixture was kept under reflux for an additional 24 h. After cooling to room temperature, the mixture was filtered and the solvent was evaporated. The crude product was purified by column chromatography (eluent petrol ether/ethyl acetate 8:1), yielding 19.7 g (0.063 mol, 69%) of colorless powder (melting point: 60 °C).

^{1}H NMR ($CDCl_3$/200 MHz): $\delta = 7.77$ (m, 2H, arom H), 7.70 (m, 2H, arom H), 3.66 (t, 2H, N−CH_2), 3.37 (t, 2H, Br−CH_2), 1.2−1.9 (m, 8H, aliphatic H).

(±)-4-Toluenesulfonic Acid 2-Octyl Ester. A solution of 90.6 mL (74.2 g/0.57 mol) of (±)-2-octanol in 300 mL of pyridine was cooled to 0 °C. Within 30 min, 104.9 g (0.55 mol) of *p*-toluenesulfonyl chloride was added. After that, the mixture was stirred for 20 h at room temperature. The reaction mixture was then poured on a mixture of 400 mL of concentrated hydrochloric acid and 600 mL of ice water. The resulting mixture was extracted three times with 300 mL of diethyl ether. The unified organic phases were dried over magnesium sulfate and filtered. After that, the solvent was evaporated in a vacuum. The reaction yielded 122.4 g of colorless oil that still contained ~10 wt % of unreacted (±)-2-octanol (equals 110.2 g/0.387 mol (±)-4-toluenesulfonic acid 2-octyl ester, yield: 70%). The product was reacted without further purification.

^{1}H NMR ($CDCl_3$, 200 MHz): $\delta = 7.73$ (d, 2H, arom H, meta to CH_3), 7.27 (d, 2H, arom H, ortho to CH_3), 4.53 (m, 1H,

RCH_2-OR), 2.39 (s, 3H, Ar−CH), 1.0−1.7 (m, 13H, aliphatic H + remaining reactant), 0.80 (t, 3H, R−CH_3 + remaining reactant).

(±)-4′-(1-Methylheptyloxy)biphenyl-4-ol (**2**)**.** A solution of 16.9 g (0.3 mol) of potassium hydroxide and 57.6 g (0.3 mol) of 4,4′-dihydroxybiphenyl in 750 mL of methanol was heated to reflux under a nitrogen atmosphere. After that, a solution of 95.6 g (0.3 mol) of (±)-4-toluenesulfonic acid-2-octyl ester prepared according to ref 37 in 160 mL of methanol was added in small portions during 8 h. The reaction mixture was then refluxed for another 40 h, and the solvent was removed in a vacuum. The residue was stirred for 1 h with 2 N hydrochloric acid, filtered, and washed twice with water and once with a small amount of ethanol. The crude product was purified by column chromatography (petrol ether/ethyl acetate 8:1). The reaction yielded 25.3 g (0.084 mol, 28%) of colorless solid (mp: 76 °C).

^{1}H NMR ($CDCl_3$, 200 MHz): δ = 7.41 (m, 4H, arom H, meta to O), 6.88 (m, 4H, arom H, ortho to O), 4.36 (m, 1H, RCH_2O-R), 3.32 (bs, 1 H, OH), 1.1−1.8 (m, 13H, aliphatic H), 0.87 (t, 3H, CH_3).

^{13}C NMR ($CDCl_3$, 50.3 MHz): δ = 157.4 (1C, arom C, ipso to −OR), 154.6 (1C, arom C, ipso to OH), 133.8 and 133.2 (2C, arom C, para to O), 127.9 and 127.7 (4C, arom C, meta to O), 116.2 and 115.6 (4C, arom C, ortho to O), 68.5 (1C, RCH_2O), 36.5, 31.8, 29.3, 25.6, 22.6, 19.8, 14.1 (7C, aliphatic C).

(±)-N-{6-[4′-(1-Methylheptyloxy)biphenyl-4-yloxy]hexyl}-phthalimide (**3**)**.** A mixture of *N*-(6-bromohexyl)phthalimide (14.05 g, 45 mmol), (±)-4′-(1-methylheptyloxy)biphenyl-4-ol (13.57 g, 45 mmol), potassium hydroxide (2.7 g, 48 mmol), and a catalytic amount of KI in 100 mL of methanol was heated to reflux for 4 days under a nitrogen atmosphere. After cooling to 4 °C, a white solid precipitated which was isolated and washed with a small amount of cool methanol. The product yielded 10.3 g (19.5 mmol, 43%) of a white solid (mp: 64 °C).

^{1}H NMR (DMSO-d_6/200 MHz): δ = 7.83 (m, 4H, arom H of phthalimide), 7.46 (d, 4H, arom H, meta to O of biphenyl), 6.91 (d, 4H, arom H, ortho to O), 4.41 (m, 1H, O−CH), 3.92 (t, 2H, O−CH_2), 3.56 (t, 2H, N−CH_2), 1.1−1.8 (m, 21H, H-6−H-9, H-19, R−CH_2), 0.81 (t, 3H, R−CH_3).

^{13}C NMR (DMSO-d_6, 50.3 MHz): δ = 167.9 (2C, carbonyl), 157.6 + 156.8 (2C, arom C, ipso to O), 134.3 (2C, arom C of phthalimide), 132.1 +132.0 (2C, arom C, para to O), 131.5 (2C, arom C of phthalimide), 127.1 + 127.0 (4C, arom C, meta to O), 122.9 (2C, arom C of phthalimide), 115.8 + 114.7 (2C, arom C, ortho to O), 72.9 (1C, O−*C*H), 67.3 (1C, O−*C*H_2), 37.3 (1C, N−*C*H_2), 35.8 (1C, O−CH−*C*H_2), 31.2 + 28.6 + 28.4 + 27.7 + 25.9 + 25.1 + 24.8 + 21.9 (8C, aliphatic C), 19.5 (1C, OCH−*C*H_3), 13.8 (1C, R−*C*H_3).

(±)-6-[4′-(1-Methylheptyloxy)biphenyl-4-yloxy]hexylamine (**4**)**.** Hydrazine hydrate (1.03 g, 20.6 mmol) was added to a solution of (±)-*N*-{6-[4′-(1-methylheptyloxy)biphenyl-4-yloxy]hexyl}-phthalimide (10.2 g, 19.2 mmol) in 100 mL of ethanol. The mixture was kept under reflux for 16 h. After addition of 10 mL of concentrated HCl, the resulting solution was kept under reflux for 1 h. After cooling to 4 °C a white solid precipitated which was isolated. The solid was stirred for 30 min in 1 M aqueous NaOH. After filtration, the crude product was heated with 200 mL of $CHCl_3$ and 5 g of Na_2SO_4 under reflux for 2 h. Filtration after cooling and evaporation of the organic solvent, the reaction yielded 4.53 g (11.3 mmol, 60%) of a white product.

^{1}H NMR ($CDCl_3$/200 MHz): δ = 7.43 (m, 4H, arom H, meta to O), 6.91 (m, 4H, arom H, ortho to O), 4.35 (m, 1H, O−C*H*), 3.96 (t, 2H, O−CH_2), 2.71 (t, 2H, NH_2−CH_2), 1.2−2.2 (m + bs, 23H, aliphatic H, NH_2), 0.87 (t, 3H, R−CH_3).

Poly(N-acryloyloxysuccinimide) was prepared as described in ref 37.

^{1}H NMR (DMSO-d_6, 200 MHz): δ = 3.11 (1H, CH, main chain), 2.80 (4H, CH_2, side groups), 2.08 (2H, CH_2, main chain).

^{13}C NMR (DMSO-d_6, 50.3 MHz): δ = 169.8 (2C, RC(O)N), 162.3 (1C, RC(O)O), 35.7 (1C, CH, main chain), 30.7 (1C, CH_2, main chain), 25.4 (2C, CH_2, side chain).

LC Homopolymer **P1.** A sample of 255 mg (1.51 mmol repeating units) of poly(*N*-acryloyloxysuccinimide) was dissolved in 40 mL of DMF and heated to 50 °C. Subsequently, a solution of 720 mg (1.81 mmol repeating units) of primary amine in 10 mL of DMF was added. The reacting mixture was stirred for 24 h at room temperature under a nitrogen atmosphere; afterward, the mixture was concentrated in a vacuum to 5 mL. The polymer was precipitated by pouring the solution into 100 mL of methanol. After centrifugation, the solvent was decanted, and the product was washed several times with methanol and dried. The reaction yielded 340 mg of a pale yellow solid.

^{1}H NMR ($CDCl_3$, 200 MHz): δ = 7.45 (4H, arom H, meta to O), 6.92 (4H, ortho to O), 4.27 (1H, O−C*H*), 3.99 (2H, NH−R−CH_2), 3.25 (2H, NH−CH_2), 1.31−1.24 (12H, aliphatic H + main chain), 0.86 (3H, O−R−CH_3).

LC Ionomers **P2.** A sample of 501 mg (2.96 mmol repeating units) of poly(*N*-acryloyloxysuccinimide) was dissolved in 40 mL of DMF and heated to 50 °C. Subsequently, a solution of 587 mg (1.48 mmol repeating units) of primary amine in 10 mL of DMF was added for **P2**. The reacting mixture was stirred for 5 h at RT under a nitrogen atmosphere. It was checked by thin-layer chromatography that no free amine was left after this time. For **P2**, a solution of 454 mg (2.96 mmol) of the 4-aminobutyric acid methyl ester hydrochloride in 10 mL of DMF was then supplemented, and then 4 mL of triethylamine was added. The mixture was stirred for a further 24 h at 50 °C. Afterward, the mixture was concentrated in a vacuum to 10 mL. The polymer was precipitated by pouring the solution into 100 mL of methanol. After centrifugation, the solvent was decanted, and the product was washed several times with methanol and dried. The reaction yielded **P2** as bright-yellow solids.

^{1}H NMR ($CDCl_3$, 200 MHz): δ = 7.41 (4H, arom H, meta to O), 6.87 (4H, ortho to O), 4.31 (1H, O−C*H*), 3.89 (2H, O−CH_2), 3.61 (3H, $COOCH_3$), 3.21 (4H, NH−CH_2), 2.31 (2H, CH_2−CH_2−$COOCH_3$), 1.71−1.23 (15H, aliphatic H + main chain), 0.86 (3H, O−R−CH_3).

IR (ATR): 2927, 2853 (C−H aliphatic), 1737 (COO−CH_3), 1644 (CO− NHR), 1497, 1238, 1173, 1035, 822 cm^{-1}.

Cleavage of the Ester Bond To Obtain LC Ionomer **P2.** A solution of 200 mg of the precursor of **P2** in 15 mL of DMF was heated to 40 °C under a nitrogen atmosphere. After that a solution of 1.1 g of potassium hydroxide in 5.5 mL of water was added to the reaction mixture with a syringe. The mixture was stirred for 5 h at 40 °C. As a white product had formed, the solvent was evaporated, and the residue was washed three times with 100 mL of water. The mixture was then centrifuged, and the solvent was decanted. The crude product was added to the solution of K_2CO_3 (pH = 9) and then again centrifuged, and the solvent was decanted. After drying, 229 mg (9.6 mmol repeating units, 72%) of a pink solid was obtained.

IR (ATR): 2928, 2856 (C−H aliphatic), 1642 (CO− NHR), 1564, 1497, 1397, 1239, 821 cm^{-1}.

P3 *LC Ionomer.* For the synthesis of **P3a** with 20% of ionic amines or **P3b** with 50% of ionic amines, 251.9 mg (1.487 mmol repeating units) of poly(*N*-acryloyloxysuccinimide) was dissolved in 15 mL of DMF and heated to 50 °C. Subsequently, a solution of 473.6 mg (1.191 mmol repeating units) of primary amine for **P3a** or 295.6 mg (0.744 mmol repeating units) of primary amine for **P3b** in 10 mL of DMF was added. The mixture was stirred for 5 h at 70 °C and then cooled to 50 °C. After that, a solution of 239 mg (0.912 mmol) of 4-aminobutyltriethylphosphonium chloride hydrochloride in 10 mL of methanol and 4 mL of triethylamine for **P3a** or 194 mg (0.744 mmol) of 4-aminobutyltriethylphosphonium chloride hydrochloride in 8 mL of methanol and 4 mL of triethylamine for **P3b** was added. The mixture was stirred for another 24 h at 50 °C. Afterward, the mixture was concentrated in a vacuum to 10 mL. The polymer was precipitated by pouring the solution into 100 mL of diethyl ether. After centrifugation, the solvent was decanted, and the product was washed several times with diethyl ether and dried. The reaction yielded **P3a** or **P3b**.

Polyelectrolytes. Branched poly(ethylenimine) (PEI) was purchased from Aldrich and used without further purification. The synthesis of poly(2-acryloylamino-2-methylpropyl sulfonate sodium salt) (PAMPS) and poly(choline methacrylate) (PCM) were already described elsewhere.[36]

Substrates for the Multilayer Buildup. The formation of multilayers was performed on a quartz glass or a silicon wafer used as substrates. Cleaning of these substrates was achieved using a classical procedure.[10] The substrates were immersed for 20 min in a 1:1 mixture of concentrated H_2SO_4 and a 30% H_2O_2 ("piranha solution"; *caution*: piranha reacts violently with organic compounds and should not be stored in closed containers) and then extensively rinsed with ultrapure water (obtained by deionization and purification using the Milli-Q system from Millipore) at three times. And then the substrates were treated with a 1:1:5 mixture of 25% aqueous NH_3, 30% H_2O_2, and H_2O at 80 °C to functionalize and thoroughly rinsed with ultrapure Milli-Q water. After further washing, the substrates were used for multilayer adsorption.

Multilayer buildup. In the beginning, two double layers of poly(ethylene imine) (PEI) (from a solution of 2.5 mg/mL PEI in 1 N hydrochloric acid) and poly(2-acryloylamino-2-methylpropyl sulfonate sodium salt) (PAMPS) (from a solution of 3.5 mg/mL PAMPS in water) were adsorbed on the substrates as basis layers. At each time, the substrates were dipped into the solution for 20 min, and then the substrates were rinsed three times with plenty of Milli-Q water (each time for 1 min) between these two steps, as already described in the literature.[1] The initially deposited double basis layers are sufficient to start the multilayer deposition process; the surface coverage and charge density appear to be more uniform after a number of bilayers of highly charged polyelectrolytes have been deposited, thereby eliminating any effects that the substrate itself may have on the adsorption process.[1] After fabrication of these basis layers, substrates were sequentially dipped in a cationic poly(choline methacrylate) (PCM) solution for 10 min (from a solution of 2.5 mg/mL PCM in water) rinsed three times by immersion in ultrapure water (1 min). And then dipped for 10 min in a polyanion solution and three times rinsing steps were performed. This deposition procedure was then cycled to obtain multilayers. The multilayers were dried under nitrogen gas purging at the end of their fabrication.

Identical procedure was adopted when the multilayers assembled by the spin-coating method. In this case, however, the polymer/solvent solution and aqueous solution of PCM were poured onto a substrate, and then the substrate was spun at a speed of 4000 rpm for 15 s. Subsequently, plenty of Milli-Q water was put on the substrate, and then the substrate was spun again at the same conditions. Before alternately depositing polymer **P2** and PCM onto the prepared substrate by the spin-coating method, PEI and PAMPS were also predeposited two times as basis layers alternately in cationic aqueous solution of PEI and then in anionic aqueous PAMPS like the solution-dipping method at same condition. The washing steps were repeated three times. At the end of every adsorption cycle, the multilayers were dried under nitrogen gas purging, and UV/vis spectra were measured.

Instruments. ^{1}H and ^{13}C NMR spectra were mostly measured on a Bruker 200 MHz FT spectrometer. In some cases spectra were also measured on a Bruker 400 MHz FT spectrometer. The spectra were analyzed with the software Win-NMR 6.1. Infrared spectra were measured on a Bruker Vector 22 FT-IR spectrometer with a Harrick ATR unit. The analysis of the spectra was performed with the software OPUS 3.1. The phase transitions temperatures of the polymers were investigated by differential scanning calorimetry (DSC) performed with a Perkin-Elmer DSC 7 at a scan rate of 10 °C min^{-1}. To determine the molecular weight of the polymers, gel permeation chromatography (GPC) was performed on a Jasco instrument and THF was used as mobile phase. The separation was done on a MZ-Gel SD plus precolumn (8 mm × 50 mm) and three MZ-Gel SD plus main columns (8 mm × 50 mm) produced by Mainz Analysentechnik. For each measurement 100 μL solution of the polymer in THF (2 mg/mL) was injected. The detection was performed with Jasco refractive index and UV detectors and a Viscotek light scattering detector. Polarizing microscopy investigations were performed with a Zeiss Jenapol SL 100 microscope. The samples were analyzed in a Linkam THMS 600 hot stage and tempered with a Linkam TMS 93-control module. X-ray measurements (LC phases) for bulk state were carried out on a Siemens D-500 diffractometer using Cu Kα radiation ($\lambda = 1.54$ Å) and a single-crystal graphite monochromator. Additionally, X-ray reflectivity measurements for multilayers were done with the setup described in ref 19.

Samples were imaged at room temperature with a commercial AFM (Nanoscope IIIa, Digital Instruments, Santa Barbara, CA) employing TappingMode using rectangular silicon cantilevers (Nanosensors, 125 μm long, 30 μm wide, 4 μm thick) with an integrated tip, a nominal spring constant of 42 N m^{-1}, and a resonance frequency of 330 kHz. To control and enhance the range of the attractive interaction regime, the instrument was equipped with a special active feedback circuit, called *Q*-control (Nanoanalytics, Germany). The quality factor *Q* of this oscillating system is increased up to 1 order of magnitude. As a consequence, the sensitivity and lateral resolution are enhanced, allowing us to prevent the onset of intermittent repulsive contact and thereby to operate the AFM constantly in the attractive interaction regime.

SPR measurements were performed in the Kretschmann configuration against ethanol. Optical coupling was achieved with a LASFN 9 prism, $n = 1.85$ at $\lambda = 632.8$ nm and index matching fluid $n = 1.70$ between prism and the BK270 glass sildes. The plasmon was excited with P-polarized radiation using a He/Ne laser (632.6 nm, 5 mW). For SPR, glass slides (3.5 cm × 2.5 cm) were used, and glass slides were cleaned with aqueous $NH_3/H_2O_2/H_2O$ (1:1:5) for 10 min at 80 °C, washed with water and 2-propanol, and dried in a stream of nitrogen. These glass slides were coated with gold using a Balzer BAE 250 vacuum coating unit under pressure of less than 5×10^{-6} hPa, typically depositing 50 nm of gold after first depositing 2 nm of Cr. The slides were exposed to 3-mercaptopropionic acid solution (1 mmol) for 12 h and then deprotonated by using 1 mmol of aqueous NaOH solution.

UV/vis measurements were performed on a Shimadzu UV-2102 PC spectrometer. Angular dependent UV/vis spectra were also examined by using the same spectrometer. A custom-built sample holder equipped with a rotation stage to which the quartz substrates were affixed was placed in the middle of the light path. Rotation of the sample holder resulted in illumination of the same area of the sample both in the parallel (0°, shear direction parallel to the electric field vector of the incident radiation) and perpendicular (90°, shear direction perpendicular to the electric field vector of the incident radiation) configurations. We performed the angular dependence of both types of samples for angles from −70° to +70°. The spectra were plotted as the absorbance at a given angle of the incident light beam; however, there is a tendency for the absorbance to increase with increase in the angle used. Above all, increasing absorption which is related to the increasing optical thickness has to be corrected by a correction factor *d*.

$$d = \frac{1}{\cos\left(\arcsin\left(\frac{\sin\theta}{1.65}\right)\right)}$$

where θ is the angle and *d* is the correction factor.

To correct for the light polarized perpendicular to the plane defined in Figure 7a (paper plane), 50% of the absorption at 0° was subtracted. This corresponds to 0.350 05 for the spin-coated sample and to 0.013 75 for the solution-dipped sample (two times this value plus the corrected absorption resulted in Figure 7b,c representing therefore the real measured absorption). The angular dependent absorption minus the 50% absorption at 0° was fitted with formula 1 from −50° to +50°. This yielded an $A_\perp$ of 0.011 44 and $A_\parallel$ of 0.028 28 for the solution-dipped sample and $A_\perp$ of 0.3484 and $A_\parallel$ of 0.4253 for the spin-coated sample. These values were used for the estimate of the order parameter.

Acknowledgment. The authors gratefully thank Hosub Kim for the help given to the SPR measurements.

Part of the work has been supported by the DFG (Ze 230/9-2).

References and Notes

(1) Ferreirat, M.; Rubner, M. F. *Macromolecules* **1995**, *28*, 7107−7114.
(2) Park, S. Y.; Rubner, M. F.; Mayes, A. M. *Langmuir* **2002**, *18*, 9600−9604.
(3) Tovar, G.; Paul, S.; Knoll, W.; Prucker, O.; Rühe, J. *Supramol. Sci.* **1995**, *2*, 89.
(4) Piscevic, D.; Knoll, W.; Tarlov, M. J. *Supramol. Sci.* **1995**, *2*, 99.
(5) Katz, H. E.; Sheller, G.; Putvinski, T. M.; Shilling, M. L.; Wilson, W. L.; Chidsey, C. E. D. *Science* **1991**, *254*, 1485.
(6) (a) Vermeulen, L. A.; Snover, J. L.; Sapochak, L. S.; Thompson, M. E. *J. Am. Chem. Soc.* **1993**, *115*, 11767. (b) Vermeulen, L. A.; Pattanayak, J.; Fisher, T.; Hansford, M.; Burgmeyer, S. *J. Mater. Res. Soc. Symp. Proc.* **1996**, *431*, 271.
(7) Rubinstein, I.; Steinberg, S.; Tor, Y.; Shanzer, A.; Sagiv, J. *Nature (London)* **1988**, *332*, 426.
(8) Li, D.-Q.; Ratner, M. A.; Marks, T. J.; Zhang, C. H.; Yang, J.; Wang, G. K. *J. Am. Chem. Soc.* **1990**, *112*, 7389.
(9) Vermeulen, L. A.; Thompson, M. E. *Nature (London)* **1992**, *358*, 656.
(10) Fou, A. C.; Onisuka, O.; Ferreira, M.; Rubner, M. F. *J. Appl. Phys.* **1996**, *79*, 7501.
(11) Decher, G.; Hong, J. D.; Schmitt, J. *Thin Solid Films* **1992**, *210/211*, 831.
(12) Dubas, S. T.; Schlenoff, J. B. *Macromolecules* **2001**, *34*, 3736.
(13) Dubas, S. T.; Schlenoff, J. B. *Macromolecules* **1999**, *32*, 8153.
(14) Schoeler, B.; Kumaraswamy, G.; Caruso, F. *Macromolecules* **2002**, *35*, 889.
(15) Steitz, R.; Jaeger, W.; Klitzing, R. v. *Langmuir* **2001**, *17*, 4471.
(16) Bertrand, P.; Jonas, A.; Laschewsky, A.; Legras, R. *Macromol. Rapid Commun.* **2000**, *21*, 319−348.
(17) Bertrand, P.; Jonas, A.; Laschewsky, A.; Legras, R. *Macromol. Rapid Commun.* **2000**, *21*, 319−348.
(18) Fischer, P.; Laschewsky, A.; Wischerhoff, E.; Arys, X.; Jonas, A.; Legras, R. *Macromol. Symp.* **1999**, *137*, 1−24.
(19) (a) Arys, X.; Laschewsky, A.; Jonas, A. M. *Macromolecules* **2001**, *34*, 3318. (b) Arys, X.; Fischer, P.; Jonas, A. M.; Koetse, M. M.; Laschewsky, A.; Legras, R.; Wischerhoff, E. *J. Am. Chem. Soc.* **2003**, *125*, 1859. (c) Glinel, K.; Jonas, A. M.; Laschewsky, A.; Vuillaume, P. Y. In *Multilayer Thin Films. Sequential Assembly of Nanocomposite Materials*; Decher, G., Schlenoff, J. B., Eds.; Wiley-VCH: Weinheim, 2003; Chapter 7, pp 177−205.
(20) Kleinfeld, E. R.; Ferguson, G. S. *Science* **1994**, *265*, 370.
(21) Kotov, N. A.; Haraszti, T.; Turi, L.; Zavala, G.; Geer, R. E.; Dékány, I.; Fendler, J. H. *J. Am. Chem. Soc.* **1997**, *119*, 6821.
(22) Kim, H. N.; Keller, S. W.; Mallouk, T. E.; Schmitt, J.; Decher, G. *Chem. Mater.* **1997**, *9*, 1414.
(23) Kotov, N. A.; Dékany, I.; Fendler, J. H. *Adv. Mater.* **1996**, *8*, 637.
(24) Cochin, D.; Passmann, M.; Wilbert, G.; Zentel, R.; Wischerhoff, E.; Laschewsky, A. *Macromolecules* **1997**, *30*, 4775.
(25) Passmann, M.; Wilbert, G.; Cochin, D.; Zentel, R. *Macromol. Chem. Phys.* **1998**, *199*, 179−189.
(26) (a) Zentel, R.; Mruk, R.; Allard, D. *Polym. Mater. Sci. Eng.* **2004**, *90*, 186−187. (b) Murk, R. Ph.D. Thesis Mainz, Germany, 2003.
(27) Cho, J.; Char, K.; Hong, J. D.; Lee, K. B. *Adv. Mater.* **2001**, *13*,*14*, 1076.
(28) Ferruti, P.; Bettelli, A.; Feré, A. *Polymer* **1972**, *13*, 462−464.
(29) Hausch, M.; Zentel, R.; Knoll, W. *Macromol. Chem. Phys.* **1999**, *200*, 174−179.
(30) Théato, P.; Zentel, R.; Schwarz, S. *Macromol. Biosci.* **2002**, *2*, 387−394.
(31) Hong, H.; Roland, S.; Kirstein, S.; Davidov, D. *Adv. Mater.* **1998**, *10*, 1104.
(32) Dubas, S. T.; Schlenoff, J. B. *Macromolecules* **1999**, *32*, 8153.
(33) Chiarelli, P. A.; Johal, M. S.; Casson, J. L.; Roberts, J. B.; Robinson, J. M.; Wang, H.-L. *Adv. Mater.* **2001**, *13*, 1167.
(34) Chiarelli, P. A.; Johal, M. S.; Holmes, D. J.; Casson, J. L.; Robinson, J. M.; Wang, H.-L. *Langmuir* **2002**, *18*, 168.
(35) Advincula, R.; Aust, E.; Meyer, W.; Knoll, W. *Langmuir* **1996**, *12*, 3536.
(36) Passmann, M.; Zentel, R. *Macromol. Chem. Phys.* **2002**, *203*, 363−374.
(37) Mruk, R.; Prehl, S.; Zentel, R. *Macromol. Chem. Phys.* **2004**, *205*, 2169−2174.
(38) Brodowsky, H. M.; Boehnke, U.-C.; Kremer, F.; Gebhard, E.; Zentel, R. *Langmuir* **1997**, *13*, 5378−5382.
(39) Vix, A.; Stocker, W.; Stamm, M.; Wilbert, G.; Zentel, R.; Rabe, J. *Macromolecules* **1998**, *31*, 9154−9159.
(40) Gebhard, E.; Zentel, R. *Liq. Cryst.* **1999**, *26*, 299−302.
(41) *Textures of Liquid Crystals, Dierking, I*; Wiley-VCH: Weinheim, 2003.
(42) *Smectic Liquid Crystals, Textures and Structures*; Gray, G. W., Goodby, J. W. G., Eds.; Leonard Hill: Glasgow, 1984.
(43) *Handbook of Liquid Crystals*; Demus, D., Goodby, J., Gray, G. W., Spiess, H.-W., Vill, V., Eds.; Wiley-VCH: Weinheim, 1998.
(44) Pohl, L. In *Liquid Crystals*; Stegemeyer, H., Ed.; Topics in Physical Chemistry; Steinkopf: Darmstadt, 1994.

MA051131T